Study of planar waveguide structure of He^{+} ion-implanted $Sn_2P_2S_6$ crystal with multiple-angle-of-incidence ellipsometry technique

[1] Kostruba A., [2] Kobec A. P., [3] Grabar A. A. and [1] Vlokh R.

[1] Institute of Physical Optics, 23 Dragomanov St., 79005 Lviv, Ukraine, vlokh@ifo.lviv.ua
[2] National Scientific Centre "Kharkiv Institute of Physics and Technology", Institute of Plasma Electronics and New Methods of Acceleration, 1 Academichna St., 61108, Kharkiv, Ukraine
[3] Institute for Solid State Physics and Chemistry, Uzhgorod National University, 54 Voloshyn St., 88000 Uzhgorod, Ukraine

Abstract

In the present work ion-implanted three-layer single-mode waveguide structure in $Sn_2P_2S_6$ crystals is obtained. The parameters of this structure are experimentally studied with the ellipsometric technique and simulated using the inverse ellipsometric problem approach. The parameters of all the layers are derived. It is found that a single-mode guiding regime can be reached for the light wavelengths belonging to the spectral region of transparency ($530\,\text{nm} < \lambda < 1279.9\,\text{nm}$). We demonstrate advantages of the ellipsometric method applied for detecting the changes occurring in the $Sn_2P_2S_6$ crystal structure due to He^{+} ion implantation.

1. Introduction

$Sn_2P_2S_6$ crystals are a prominent representative of wide-gap semiconductors. They represent a basic compound for creating solid solutions with a general formula $Sn_2P_2(Se_xS_{1-x})_6$, which are extensively studied in recent years. The crystals are interesting from different points of view: critical behaviour near the phase transition points [1–3], extremely high electro-, magneto- and acoustooptic parameters [4–8], promising photorefractive properties [9, 10], etc.

Under atmospheric pressure $Sn_2P_2S_6$ crystals reveal a proper ferroelectric phase transition with the change of point symmetry group $2/m \leftrightarrow m$ (the Curie point $T_c = 337\,\text{K}$) [1]. The crystals are known as highly efficient electrooptic material, with the electrooptic parameter $r_{11} = 1.74 \times 10^{-10}$ m/V at the room temperature and the light wavelength of $\lambda = 632.8\,\text{nm}$ [4, 5]. $Sn_2P_2S_6$ represents also a promising magnetooptic

(the Verdet constant being equal to $115 \, \text{rad/T} \times \text{m}$ [6]) and acoustooptic material. Therefore accomplishing of optical planar waveguides on its basis, with suitable optical parameters, would be very promising for efficient operation of laser radiation in many integrated optical applications.

It has been shown in the work [11] that using of He^+ ion implantation method allows creating planar waveguides on the basis of $Sn_2P_2S_6$ crystals. Differences between the refractive indices of substrate and guiding layers as large as $\Delta n = 0.14$ and $\Delta n = 0.07$ have been obtained for the fluences $2 \times 10^{15} \, \text{cm}^{-2}$ and $0.5 \times 10^{15} \, \text{cm}^{-2}$, respectively, and the energy of $2 \, \text{MeV}$ [11]. In these experiments, the sample surface has been kept tilted by 7 deg with respect to the normal incidence of an ion beam in order to avoid a channelling effect. As a result, a multimode waveguide layer with the average thickness of $\sim 6 \, \mu\text{m}$ has been obtained, which supports propagation of He-Ne laser radiation ($\lambda = 632.8 \, \text{nm}$). However, the authors [11] have not found the lowest energy of the ion beam which is needed for creating single-mode waveguide based on $Sn_2P_2S_6$ crystals.

The goal of the present work is to solve this problem with applying an ellipsometric technique. Notice that solving exactly a so-called inverse ellipsometric problem and determining accurately the refractive indices of $Sn_2P_2S_6$ is very difficult [12, 13], since the latter crystal is optically biaxial, with the monoclinic point symmetry *m*.

2. Experimental

$Sn_2P_2S_6$ crystals were grown by a vapour transport technique. Since they belong to the monoclinic point group, the crystallographic coordinate system is not orthogonal though the deviation from orthogonality of *a* and *c* axes is small enough ($1.15°$ – see [14]). As a result, we will neglect this non-orthogonality and below we will refer to the crystallographic system a, b, c as an orthogonal one. Crystal samples were prepared in the shape of parallelepipeds, with the average dimensions of $2 \times 5 \times 7 \, \text{mm}^3$, flat parallel faces perpendicular to the *c* direction, and lateral faces parallel to the *a* and *b* axes. The lattice parameters under normal conditions are equal to $a = 0.9378 \, \text{nm}$, $b = 0.7448 \, \text{nm}$, $c = 0.6513 \, \text{nm}$ and $\beta = 91.15°$ (see, e.g., [14]). Here the *b* axis is perpendicular to the symmetry mirror plane, while the *a* axis is almost parallel to the spontaneous polarisation vector. In other words, the *a* and *b* axes in our setting are defined in a purely crystallographic sense, while the *c* axis is perpendicular to the *ab* plane.

The He^+ ion implantation was performed using a linear accelerator of multi-charged ions, MILAC. During the ion implantation doping process, the ions of He^+ dopant were generated and then accelerated to the energy of 1.8 MeV at the fluence of $0.5 \times 10^{15} \, \text{cm}^{-2}$, before impinging on a substrate. The process was carried out in a vacuum at the conditions of normal incidence of ions at the substrate.

Approximate equations for determination of optical parameters of anisotropic media have been suggested in the works [12, 13]. These approximations may be used while

estimating the refractive indices of the low-symmetry $Sn_2P_2S_6$ crystals. Two parameters can be determined following from standard ellipsometric measurements on the c-faced crystal cuts. These are the refractive index $n_2 = n_b$ and the birefringence Δn. Notice that the Δn parameter does not represent a principal value of the birefringence since the Fresnel ellipsoid is rotated by the angle of ~ 45 deg around the b axis.

Two independent ellipsometric measurements were performed for each angle of incidence (IA): the first one for the plane bc of light incidence, in order to determine the complex reflectance ratio $\rho_{\parallel} = \tan \Psi_{\parallel} \exp\left(i\Delta_{\parallel}\right)$, and the second one for the orthogonal plane ac, to determine the reflectance ratio $\rho_{\perp} = \tan \Psi_{\perp} \exp\left(i\Delta_{\perp}\right)$. Here $\Psi_{\parallel}$, $\Psi_{\perp}$ and $\Delta_{\parallel}$, $\Delta_{\perp}$ are the amplitude and phase ellipsometric parameters, respectively. The refractive index value n_2 may be calculated from the relation

$$n_2 = n_y = \sin\varphi \sqrt{1 + \frac{\left(1-\rho_0\right)^2}{\left(1+\rho_0\right)^2}\tan^2\varphi} \, , \tag{1}$$

where $\rho_0 = \rho_{\parallel}(1 - B\Delta n)$, while the birefringence is given by

$$\Delta n = \frac{\delta}{k} = \frac{1}{k}\left(1 - \frac{\rho_{\parallel}}{\rho_{\perp}}\right). \tag{2}$$

The parameters denoted henceforth as B and k may be determined for the experimental geometry and conditions described in the study [13]. In our case they are as follows:

$$k = \frac{2R^2\left(1+\cos^2\varphi\right)}{\sqrt{R^2-1}\left(1-R^2\sin^2\varphi\right)\left(1-R^2\cos^2\varphi\right)},$$
$$B = \frac{2R\left(R^2-1\right)\cos\varphi}{\sqrt{R^2-1}\left(1-R^2\sin^2\varphi\right)\left(1-R^2\cos^2\varphi\right)}, \tag{3}$$

where $R = \sqrt{1 + \frac{\left(1-\rho_{\parallel}\right)^2}{\left(1+\rho_{\parallel}\right)^2}\tan^2\varphi}$ is determined by the ellipsometric parameters and φ is the IA. Therefore, the principal refractive index (n_2) and the birefringence (Δn) may be found from the ellipsometric parameters measured for the general bc plane of light incidence and the orthogonal ac plane. It is obvious that the quantity $\delta = \left(1 - \rho_{\parallel}/\rho_{\perp}\right)$ is a measure of the optical anisotropy.

Optimal experimental conditions for the ellipsometric experiments depend upon a lot of parameters. So, the measurements will have the maximal sensitivity for the case of principal IA when the phase ellipsometric parameter Δ of the system under test is equal to $\pi/2$ or $3\pi/2$. For our crystal, the principal IA is approximately equal to $70\,\text{deg}$. However, the data obtained under these conditions are distorted most of all, too. The

distortions are caused by a presence of surface layer (SL) associated with the mechanical polishing process [15, 16]. Therefore the IA region suitable for obtaining the most accurate results is shifted towards smaller angles ($65 \div 67$ deg).

3. Results and discussion
3.1. Ellipsometric investigation of planar waveguide structure. Isotropic approximation

Using the data of ellipsometric experiments performed at different IAs, we have obtained the refractive indices and the birefringence for the c-faced $Sn_2P_2S_6$ crystals. They are as follows: the principal refractive index $n_2 = 2.93 \pm 0.01$, the non-principal index $n_x = 3.05 \pm 0.01$, and $\Delta n = 0.12$. Notice that these results agree well with those derived earlier with the prism method ($n_2 = 2.9309$ and $n_x = 3.0629$ [17]).

In order to determine the parameters of the SL, the ellipsometric data obtained in the vicinity of the principal IA ($69 \div 70$ deg) may be used. In this case a single-layer model of the surface in isotropic approximation has been employed. We have found that the best agreement between the experimental and simulated data occurs for the layer parameters $d_1 = 23.7$ nm and $N_1 = 2.185 - i0.001$, where N_1 is the complex refractive index (like in the case of the layer thicknesses, here the subscripts correspond to the sequence numbers of layers and, in particular, the upper layer (the air) is denoted by the subscript 'zero').

Using the ellipsometric data obtained for the implanted surface in the two orthogonal incidence planes and the calculation procedure described above (see Eqs. (1) and (2)), we have calculated the optical parameters of the He^{+}-implanted sample. The refractive indices and the birefringence of the implanted sample are as follows: $n_2' = 2.98 \pm 0.01$, $n_x' = 3.02 \pm 0.01$ and $\Delta n = 0.04$. It is evident that the surface He^{+} ion implantation cannot change the refractive indices and the birefringence in all the volume of a bulk sample. Hence, the values obtained above do not reflect the whole real situation. Nonetheless, decrease in the anisotropy of the implanted layer ($\Delta n \approx 3\Delta n'$) testifies that the implantation process causes considerable structural changes in the surface layer. This may be explained by lattice disordering in the region of the surface layer. As one can see, the implantation leads to considerable decrease in the birefringence. That is why we will further use isotropic approximation in order to simplify our consideration.

Let us now consider a surface model according to which the surface consists of three isotropic layers. The structure of this model is presented schematically in Fig. 1. The model is as follows. The SL is located on the top of the structure. The parameters of this layer (d_1, N_1) depend only on the conditions of polishing treatment. They have been determined above.

The waveguide core layer (WCL) is located in the middle of the structure. The thickness of this layer depends upon the implantation energy of He^{+} ions. In accordance with the "Stopping and Range of Ions in Matter" (SRIM) simulation procedure [18], the

Fig. 1. Three-layer model of waveguide structure on the surface of $Sn_2P_2S_6$ crystal: the SL denotes the surface layer, the WCL the waveguide core layer and the IBL the implanted barrier one.

maximum recoil energy transferring occurs at the depth of about $6\,\mu m$ (the sum thickness of the SL and WCL) for the implantation energy of 1.8 MeV [11]. According to the work [11], the refractive index in the core region is only slightly increased ($N_2 = 3.05 + 0.006$) by the implantation. Thus, we can use the values $N_2 \approx 3.05$ and $d_2 = 6\,\mu m$ in our calculation. The implanted barrier layer (IBL) is located in the bottom of the model structure. Following the idea presented in the study [19], the change in optical parameters and the thickness of the third layer caused by the energy deposition $G_n(z) = dE/dz$ and the implantation fluence Φ is given by

$$\Delta n(z) = \Delta n_0 \left(1 - \exp\left(-\Phi G_n(z)/G_0\right)\right), \tag{4}$$

where Δn_0 and G_0 are fitting parameters. For the implantation fluence of $0.5 \times 10^{15}\,\text{cm}^{-2}$, the maximum refractive index change is about $\Delta n_{max} = -0.07$. The index profile remains flat for the depths of about 500 nm in this barrier region [11]. Therefore this region can be modelled as the IBL, with the thickness $d_3 = 500\,\text{nm}$ and the refractive index $N_3 = n_x - \Delta n_{max} = 3.05 - 0.07 = 2.98$. Then the models of the implanted multilayer crystal surface, as well as the surface before implantation, are fully defined in the isotropic approximation and so they can be used in the simulation experiment when solving the direct ellipsometry problem. In other words, the polarisation parameters of the reflected light (the dependences of the ellipsometric parameters Δ, Ψ upon the IA φ) for the surface structures described here are defined in all the range of φ values. Now, the experimental data obtained for a wide IA range may be compared with the results of our simulation.

The experimental and simulated ellipsometric data for the non-implanted sample are presented in Fig. 2. As one can easily see, the simulation results agree well with the experimental data. This demonstrates a real equivalence between the monolayer model and the real surface.

The situation appearing under ellipsometric study of the implanted crystal surface is essentially different (see Fig. 3). Here disagreement between the experimental and the

calculated dependences is obvious, thus demonstrating differences of the model considered above and the real state of the surface.
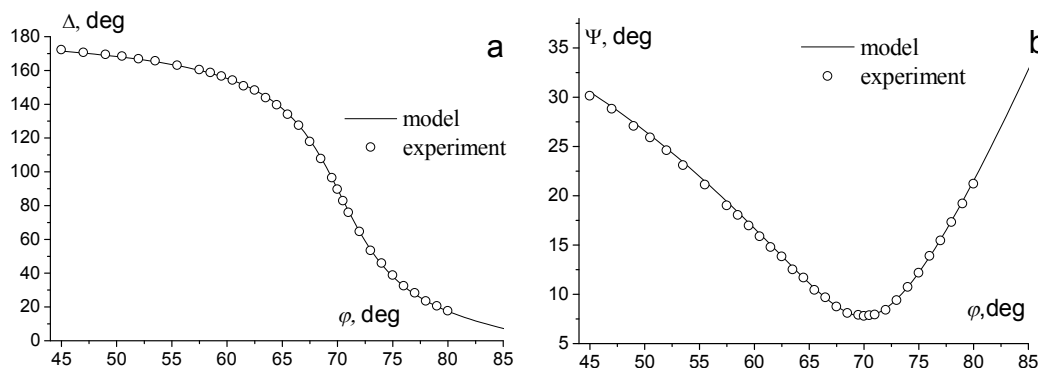
Fig. 2. Angular dependences of the ellipsometric parameters $\Delta(\varphi)$ (a) and $\Psi(\varphi)$ (b): circles are the experimental data and solid curves the results of simulation using a monolayer surface model "crystal–SL". The parameters of the surface model are $d_1 = 23.7$ nm and $N_1 = 2.185 - i \times 0.001$, whereas $N_c = 3.05$ is the refractive index of the bulk crystal.
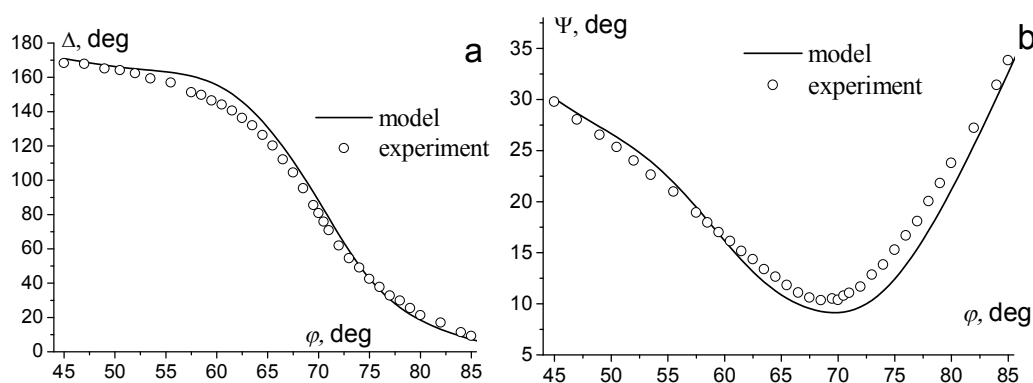
Fig. 3. Angular dependences of the ellipsometric parameters $\Delta(\varphi)$ (a) and $\Psi(\varphi)$ (b): circles are the experimental data and solid curves the result of simulation using a three-layer surface model "crystal–WCL–SL–IBL" (cf. Fig. 1). The parameters of the surface model are $d_1 = 23.7$ nm and $N_1 = 2.185 - i \times 0.001$ for the SL, $d_2 = 6$ μm and $N_2 = 3.05$ for the WCL, $d_3 = 500$ nm and $N_3 = 2.98$ for the IBL, whereas $N_c = 3.05$ is the refractive index of the bulk crystal.

The features mentioned above mean that one should solve an inverse ellipsometry problem and thus create a new surface model that must agree with the experimental data. It is obvious that the thickness and the optical parameters of the SL should be left the same, because no mechanical treatment has not been carried out after the implantation process. The optical parameters of the WCL are practically independent of the implantation characteristics and should be remained unchanged, too.

SL d_1, N_1	SL d_1, N_1	SL d_1, N_1
WCL d_2=295nm , N_2=3.05	WCL d_2=520nm , N_2=3.05	
IBL d_3=530nm , N_3=2.88		WCL $d_2 = 970$nm , N_2=3.05
	IBL d_3=515nm , N_3=2.88	
		IBL d_3=505nm , N_3=2.86
Bulk crystal	Bulk crystal	Bulk crystal
model (1	model (2	model (3

Fig. 4. Three-layer surface models obtained using the fitting procedure: d_2, d_3 and $N_3 = n_3 - ik_3$ are the floating parameters of the models.

As a consequence, the four quantities are to be considered as the fitting parameters of the model under consideration. These are the thicknesses of the WCL and the IBL (d_2 and d_3) and the complex refractive index of the IBL ($N_3 = n_3 - ik_3$) that depends on the two real parameters (the refractive index n_3 and the extinction coefficient k_3 of the IBL). Such a large quantity of unknown (floating) parameters needs increasing volume of experimental information. To solve the problem, we have used seven pairs of experimental ellipsometric angles Δ and Ψ taken from the overall IA range.

The ellipsometric data have been fitted using a standard procedure of minimising the square deviation χ between the measured (Δ_{ms} and Ψ_{ms}) and the calculated (Δ_{cl} and Ψ_{cl}) ellipsometric parameters:

$$\chi = \frac{1}{2n-m-1}\sum_{i=1}^{n}\left[\left(\Delta_{cl}^{i} - \Delta_{ms}^{i}\right)^2 + \left(\Psi_{cl}^{i} - \Psi_{ms}^{i}\right)^2\right]. \tag{5}$$

Here n means a number of the IAs (i.e., a number of different experimental situations) and m a number of the floating parameters to be fitted.
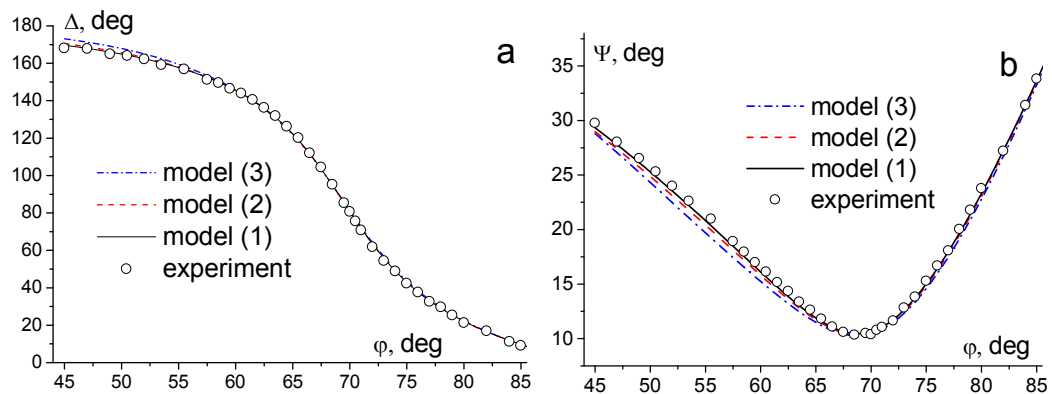
Fig. 5. Angular dependences of the ellipsometric parameters $\Delta(\varphi)$ (a) and $\Psi(\varphi)$ (b): circles are the experimental data and solid, dashed and dot-and-dash curves correspond respectively to the models (1), (2) and (3).

Three models of the implanted surface, which reveal quite similar ellipsometric responses, have been obtained as a result of solving the inverse problem. The structure of those models of the surface is presented schematically in Fig. 4.

The corresponding dependences of the ellipsometric parameters on the IA are shown in Fig. 5. It is seen that the surface model (1) involving the thinnest WCL ($d_3 = 0.295\,\mu\text{m}$) seems to be the most close to the experimental data. Moreover, increasing WCL thickness leads to essential disagreement between the measured and the calculated ellipsometric parameters, especially in the IA region extending from 45 to 60 deg.

3.2. Estimation of waveguiding effect

Verification of a possibility for waveguiding along the *b* or *a* axes in the planar waveguide implanted due to the fluence $\Phi = 0.5 \times 10^{15}\,\text{cm}^{-2}$ is another general goal of the present work. As a matter of fact, the waveguide obtained by us is asymmetric, since one can neglect thin SL. Then the propagating modes would be confined by the air ($n_0 = 1$) and the IBL ($n_2 = 3.05$), while the thickness of the guiding layer may be written as $d = d_1 + d_2 = 318.7\,\text{nm}$. It is well known that the cut-off condition for the asymmetric waveguides is given by the relation [20]

$$\Delta n = n_2 - n_3 > \frac{(2m+1)^2 \lambda_0^2}{16(n_2 + n_3)d^2} ,$$ (6)

where λ_0 is the light wavelength in vacuum. It follows from Eq. (6) that the wavelength under interest should be less than 1279.9 nm in order for the zero-order mode to be propagated, while for the first-order mode it should be less than 426.6 nm. Notice that the absorption edge of $Sn_2P_2S_6$ corresponds to the wavelength of 530 nm. The thickness of the guiding layer needed for supporting of zero-order mode propagation at the wavelength of 632.8 nm is as small as 157.56 nm.

Conclusions

As a result of the present studies, we have obtained ion-implanted three-layer structure of $Sn_2P_2S_6$ crystals. Under the condition of normal incidence of He^+ ion-implanted beam (the energy of 1.8 MeV and the fluence of $0.5 \times 10^{15}\,\text{cm}^{-2}$) we have created a three-layer structure based upon the $Sn_2P_2S_6$ crystals. Namely, we have got the SL characterised with the parameters $d_1 = 23.7\,\text{nm}$ and $N_1 = 2.185 - i \times 0.001$, the WCL with the parameters $d_2 = 295\,\text{nm}$ and $N_2 = 3.05$, and the IBL with $d_3 = 530\,\text{nm}$ and $N_3 = 2.88$. The planar waveguide obtained by us turns out to be single-mode. It has also been found that the single-mode guiding regime can be reached for the light wavelengths $530\,\text{nm} < \lambda < 1279.9\,\text{nm}$ belonging to the transparency range of $Sn_2P_2S_6$. The thickness of the guiding layer needed for supporting zero-order mode propagation is as small as 157.56 nm when the wavelength of 632.8 nm is used. We have additionally shown that

the ellipsometric method reveals some advantages, when compare with the method used in [11], when being applied to the problem of detection of changes in the $Sn_2P_2S_6$ crystal structure appearing as a result of He^+ ion implantation.

References

1. Slyvka V Yu and Vysochanskii Yu M, Ferroelectrics of $Sn_2P_2S_6$ family properties around the Lifshitz point. Uzhgorod: Zakarpattya, 1994.

2. Vysochanskii Y M, Janssen T, Currat R, Folk R, Banys J, Grigas J and Samulionis V, Phase transitions in ferroelectric phosphorous chalcogenide crystals. Vilnius: University Publishing House, 2006.

3. Gerzanich E I, 2008. Optical Properties of $A_2^{IV}B_2^{V}C_6^{VI}$ ferroelectrics-semiconductors: the effect of temperature and hydrostatic pressure. Ukr. J. Phys. Opt. **9**: 129–162.

4. Vlokh R O, Vysochanskii Yu M, Grabar A A, Kityk A V and Slivka V Yu, 1991. Electrooptic effect in $Sn_2P_2S_6$ ferroelectrics. Izv. Akad. Nauk SSSR, Ser. Neorg. Mater. **27**: 689–692.

5. Haertle D, Caimi G, Haldi A, Montemezzani G, Günter P, Grabar A A, Stoika I M and Vysochanskii Yu M, 2003. Electro-optical properties of $Sn_2P_2S_6$. Opt. Commun. **215**: 333–343.

6. Krupych O, Adamenko D, Mys O, Grabar A and Vlokh R, 2008. Faraday effect in $Sn_2P_2S_6$ crystals. Appl. Opt. **47**: 6040–6045.

7. Martynyuk-Lototska I Yu, Mys O G, Grabar A A, Stoika I M, Vysochanskii Yu M and Vlokh R O, 2008. Highly efficient acoustooptic diffraction in $Sn_2P_2S_6$ crystals. Appl. Opt. **47**: 52–55.

8. Mys O, Martynyuk-Lototska I, Grabar A, Vysochanskii Yu and Vlokh R, 2006. Piezooptic coefficients and acoustic wave velocities in $Sn_2P_2S_6$ crystals. Ukr. J. Phys. Opt. **7**: 124–128.

9. Odoulov S G, Shumelyuk A N, Hellwig U, Rupp R, Grabar A A and Stoyka I M, 1996. Photorefraction in tin hypothiodiphosphate in the near infrared. J. Opt. Soc. Amer. B **13**: 2352–2360.

10. Jazbinsek M, Montemezzani G, Gunter P, Grabar A A, Stoika I M and Vysochanskii Y. M, 2003. Fast near-infrared self-pumped phase conjugation with photorefractive $Sn_2P_2S_6$. J. Opt. Soc. Amer. B. **20**: 1241–1256.

11. Guarino A, Jazbinsek M, Herzog C, Degl'Innocenti R, Poberaj G and Gunter P, 2006. Optical waveguides in $Sn_2P_2S_6$ by low fluence MeV He^+ ion implantation. Opt. Express. **14**: 2344–2358.

12. Graves R H W, 1969. Determination of the optical constants of anisotropic crystals. J. Opt. Soc. Amer. **59**: 1225–1227.

13. Filipov VV, Tronin AYu and Konstantinova AF, 1994. Ellipsometry of anisotropic media. Kristallografiya, **39**: 360–382.

14. Dittmar G and Schaffer H, 1974. The crystal structure of $Sn_2P_2S_6$. Z. Naturforsch. B **29**: 312–317.

15. Soe-Mie F Nee, 1988. Ellipsometric analysis for surface roughness and texture. Appl. Opt. **27**: 2819–2831.

16. Collins R W, Joohyun Koh, Fujiwara H, Rovira P I, Ferlauto A S, Zapien J A, Wronski C R and Messie R, 2000. Recent progress in thin film growth analysis by multichannel spectroscopic ellipsometry. Appl. Surf. Sci., **154–155**: 217–228.

17. Haertle D, Guarino A, Hajfler J, Montemezzani G and Gunter P, 2005. Refractive indices of $Sn_2P_2S_6$ at visible and infrared wavelengths. Opt. Express. **13**: 2047–2057.

18. www.srim.org

19. Fluck D, Jundt D H, Gunter P, Fleuster M and Buchal Ch, 1993. Modelling of refractive index profiles of He^+ ion implanted $KNbO_3$ waveguides based on the irradiation parameters. J. Appl. Phys. **74**: 6023–6031.

20. Hunsperger RG, Integrated optics: theory and technology. 5th ed., Berlin, Heidelberg, New-York: Springer-Verlag, 2002.

Анотація. *У даній роботі отримано іонно-імплантовані, трьохшарові, одномодові хвилеводи на основі кристалів $Sn_2P_2S_6$. Параметри цих структур експериментально досліджені еліпсометричним методом та промодельовані розв'язуванням оберненої еліпсометричної задачі. Отримані параметри для всіх трьох шарів. Встановлено, що одномодовий хвилеводний режим може реалізуватись для довжин хвиль оптичного випромінювання 530нм<λ<1279,9нм, що належать до області прозорості кристалу. Продемонстровані переваги еліпсометричного методу при встановленні змін, які виникають в кристалах $Sn_2P_2S_6$ при іонній імплантації іонами He^+.*